Data Fusion Improves the Coverage of Wireless Sensor Networks

Guoliang Xing[1]; Rui Tan[2]; Benyuan Liu[3]; Jianping Wang[2]; Xiaohua Jia[2]; Chih-Wei Yi[4]

[1]Department of Computer Science & Engineering, Michigan State University, USA
[2]Department of Computer Science, City University of Hong Kong, HKSAR
[3]Department of Computer Science, University of Massachusetts Lowell, USA
[4]Department of Computer Science, National Chiao Tung University, Taiwan

glxing@msu.edu; {tanrui2@student., jianwang@, csjia@}cityu.edu.hk;
bliu@cs.uml.edu; yi@cs.nctu.edu.tw

ABSTRACT

Wireless sensor networks (WSNs) have been increasingly available for critical applications such as security surveillance and environmental monitoring. An important performance measure of such applications is *sensing coverage* that characterizes how well a sensing field is monitored by a network. Although advanced *collaborative* signal processing algorithms have been adopted by many existing WSNs, most previous analytical studies on sensing coverage are conducted based on overly simplistic sensing models (*e.g.*, the disc model) that do not capture the stochastic nature of sensing. In this paper, we attempt to bridge this gap by exploring the fundamental limits of coverage based on stochastic *data fusion* models that fuse *noisy* measurements of multiple sensors. We derive the scaling laws between coverage, network density, and signal-to-noise ratio (SNR). We show that data fusion can significantly improve sensing coverage by exploiting the collaboration among sensors. In particular, for signal path loss exponent of k (typically between 2.0 and 5.0), $\rho_f = \mathcal{O}(\rho_d^{1-1/k})$, where ρ_f and ρ_d are the densities of uniformly deployed sensors that achieve full coverage under the fusion and disc models, respectively. Our results help understand the limitations of the previous analytical results based on the disc model and provide key insights into the design of WSNs that adopt data fusion algorithms. Our analyses are verified through extensive simulations based on both synthetic data sets and data traces collected in a real deployment for vehicle detection.

Categories and Subject Descriptors

C.2.1 [**Computer-Communication Networks**]: Network Architecture and Design—*Network topology*; G.3 [**Probability and Statistics**]: Stochastic processes

MobiCom'09, September 20–25, 2009, Beijing, China.

General Terms

Performance, Theory

Keywords

Data fusion, target detection, coverage, performance limits, wireless sensor network

1. INTRODUCTION

Recent years have witnessed the deployments of wireless sensor networks (WSNs) for many critical applications such as security surveillance [16], environmental monitoring [25], and target detection/tracking [21]. Many of these applications involve a large number of sensors distributed in a vast geographical area. As a result, the cost of deploying these networks into the physical environment is high. A key challenge is thus to predict and understand the expected sensing performance of these WSNs. A fundamental performance measure of WSNs is *sensing coverage* that characterizes how well a sensing field is monitored by a network. Many recent studies are focused on analyzing the coverage performance of large-scale WSNs [4, 19, 24, 33, 38, 41, 43].

Despite the significant progress, a key challenge faced by the research on sensing coverage is the obvious discrepancy between the advanced information processing schemes adopted by existing sensor networks and the overly simplistic sensing models widely assumed in the previous analytical studies. On the one hand, many WSN applications are designed based on *collaborative* signal processing algorithms that improve the sensing performance of a network by jointly processing the noisy measurements of multiple sensors. In practice, various stochastic *data fusion* schemes have been employed by sensor network systems for event monitoring, detection, localization, and classification [8, 10, 11, 16, 20, 21, 29, 34]. On the other hand, collaborative signal processing algorithms such as data fusion often have complex complications to the network-level sensing performance such as coverage. As a result, most analytical studies[1] on sensing coverage are conducted based on *overly simplistic* sensing models [3, 4, 14, 18, 19, 23, 24, 33, 38, 39, 43]. In particular, the

[1]Among the total six papers on the coverage problem of WSNs that have been published at MobiCom since 2001, five of them adopted the disc sensing model. Similarly, the disc model is also assumed by seven out of nine relevant papers published at MobiHoc since 2001.

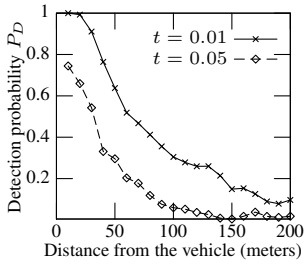

Figure 1: Detection probability *vs.* the distance from the vehicle.

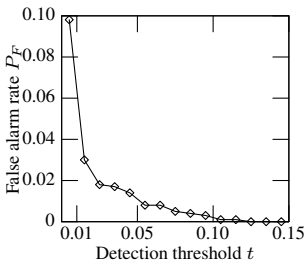

Figure 2: False alarm rate *vs.* detection threshold.

sensing region of a sensor is often modeled as a disc with radius r centered at the position of the sensor, where r is referred to as the *sensing range*. A sensor *deterministically* detects the targets (events) within its sensing range. Although such a model allows a geometric treatment to the coverage problem, it fails to capture the stochastic nature of sensing.

To illustrate the inaccuracy of the disc sensing model, we plot the sensing performance of an acoustic sensor in Fig. 1 and 2 using the data traces collected from a real vehicle detection experiment [1]. In the experiment, the sensor detects moving vehicles by comparing its signal energy measurement against a threshold (denoted by t). Fig. 1 plots the probability that the sensor detects a vehicle (denoted by P_D) versus the distance from the vehicle. No clear cut-off boundary between successful and unsuccessful sensing of the target can be seen in Fig. 1. Similar result is observed for the relationship between the sensor's false alarm rate (denoted by P_F) and the detection threshold shown in Fig. 2. Note that P_F is the probability of making a positive decision when *no* vehicle is present.

In this work, we develop an analytical framework to explore the fundamental limits of coverage of large-scale WSNs based on stochastic data fusion models. To characterize the inherent stochastic nature of sensing, we propose a new coverage measure called (α, β)-coverage where α and β are the upper and lower bounds on the system false alarm rate and detection probability, respectively. Compared with the classical definition of coverage, (α, β)-coverage explicitly captures the performance requirements imposed by sensing applications. For instance, the full $(0.05, 0.9)$-coverage of a region ensures that the probability of detecting any event occurring in the region is no lower than 90% and no more than 5% of the network reports are false alarms.

The main focus of this paper is to investigate the fundamental scaling laws between coverage, network density, and signal-to-noise ratio (SNR). To the best of our knowledge, this work is the first to study the coverage performance of large-scale WSNs based on collaborative sensing models. Our results not only help understand the limitations of the existing analytical results based on the disc model but also provide key insights into designing and analyzing the large-scale WSNs that adopt stochastic fusion algorithms. The main contributions of this paper are as follows.

- We derive the (α, β)-coverage of random networks under both data fusion and probabilistic disc models. Based on these results, we can compute the minimum network density that is required to achieve a desired level of sensing coverage. Moreover, the existing analytical results based on the disc model can be naturally extended to the context of stochastic event detection.
- We study the fundamental scaling laws of (α, β)-coverage. Let ρ_d and ρ_f denote the minimum network densities for achieving full coverage under the disc and fusion models, respectively. We prove that $\rho_f = \mathcal{O}(\frac{2r^2}{R^2} \cdot \rho_d)$ where r is the radius of sensing disc and R is the fusion range within which the measurements of all sensors are fused[2]. As fusion range can be much greater than sensing range, ρ_f is much smaller than ρ_d. Furthermore, when the optimal fusion range is adopted, $\rho_f = \mathcal{O}(\rho_d^{1-1/k})$ where k is the signal's path loss exponent that typically ranges from 2.0 to 5.0. In particular, when $k = 2$ (which typically holds for acoustic signals), $\rho_f = \mathcal{O}(\sqrt{\rho_d})$. This result shows that data fusion can effectively reduce the network density compared with the disc model. Furthermore, the existing analytical results based on the disc model significantly overestimate the network density required for achieving coverage.
- We study the impact of signal-to-noise ratio (SNR) on the network density when full coverage is required. We prove that $\rho_f/\rho_d = \mathcal{O}(\text{SNR}^{2/k})$. This result suggests that data fusion is more effective in reducing the density of low-SNR network deployments, while the disc model is suitable only when the SNR is sufficiently high.
- To verify our analyses, we conduct extensive simulations based on both synthetic data sets and real data traces collected from 20 sensors. Our simulations show that our analytical results can accurately predict the stochastic coverage of WSNs under a variety of realistic settings.

The rest of this paper is organized as follows. Section 2 reviews related work. Section 3 introduces the background and problem definition. We study the (α, β)-coverage under the disc and fusion models in Section 4 and 5, respectively. In Section 6, we investigate the impact of data fusion on asymptotic sensing coverage. Section 7 presents simulation results and Section 8 concludes this paper.

2. RELATED WORK

Many sensor network systems have incorporated various data fusion schemes to improve the system performance. In the surveillance system based on MICA2 motes [16], the system false alarm rate is reduced by fusing the detection decisions made by multiple sensors. In the DARPA SensIT project [1], advanced data fusion techniques have been employed in a number of algorithms and protocols designed for target detection [8, 21], localization [20, 34], and classification [10, 11]. Despite the wide adoption of data fusion in practice, the performance analysis of large-scale fusion-based WSNs has received little attention.

There is a vast of literature on stochastic signal detection based on multi-sensor data fusion. Early works [5, 37]

[2]We adopt the following asymptotic notation: 1) $f(x) = \mathcal{O}(g(x))$ means that $g(x)$ is the asymptotic upper bound of $f(x)$; 2) $f(x) = \Theta(g(x))$ means that $g(x)$ is the asymptotic tight bound of $f(x)$.

focus on small-scale powerful sensor networks (*e.g.*, several radars). Recent studies on data fusion have considered the specific properties of WSNs such as sensors' spatial distribution [10, 11, 29] and limited sensing/communication capability [8]. However, these studies focus on analyzing the optimal fusion strategies that maximize the system performance of a given network. In contrast, this paper explores the fundamental limits of sensing coverage of WSNs that are designed based on existing data fusion strategies. Recently, irregular sampling theory has been applied for reconstructing physical fields in WSNs [30,31]. Different from these works that focus on developing sampling schemes to improve the quality of signal reconstruction, we aim to analyze sensors' spatial density for achieving the required level of coverage.

As one of the most fundamental issues in WSNs, the coverage problem has attracted significant research attention. Previous works fall into two categories, namely, coverage maintenance algorithms/protocols and theoretical analysis of coverage performance. These two categories are reviewed briefly as follows, respectively.

Early work [22, 26, 27] quantifies sensing coverage by the length of target's path where the accumulative observations of sensors are maximum or minimum [22, 26, 27]. However, these works focus on devising algorithms for finding the target's paths with certain level of coverage. Several algorithms and protocols [41, 42] are designed to maintain sensing coverage using the minimum number of sensors. However, the effectiveness of these schemes largely relies on the assumption that sensors have circular sensing regions and deterministic sensing capability. Several recent studies [2, 17, 32, 40] on the coverage problem have adopted probabilistic sensing models. The numerical results in [40] show that the coverage of a network can be expanded by the cooperation of sensors through data fusion. However, these studies do not quantify the improvement of coverage due to data fusion techniques. Different from our focus on analyzing the fundamental limits of coverage in WSNs, all of these studies aim to devise algorithms and protocols for coverage maintenance.

Theoretical studies of the coverage of large-scale WSNs have been conducted in [4, 14, 18, 19, 23, 24, 33, 38, 43]. Most works [18, 19, 23, 33, 38, 43] focus on deriving the asymptotic coverage of WSNs. The critical conditions for full k-coverage (*i.e.*, any physical point is within the sensing range of at least k sensors) over a bounded square area [19, 33, 38, 43] or barrier area [18,23] are derived for various sensor deployment strategies. The coverage of randomly deployed networks is studied in [24]. The existing theoretical results on coverage for both static and mobile sensors/targets are surveyed in [4]. However, all the above theoretical studies are based on the deterministic disc model. In this paper, we compare our results obtained under a data fusion model against the results from [4, 24].

3. BACKGROUND AND PROBLEM DEFINITION

In this section, we first describe the preliminaries of our work, which include sensor measurement, network, and data fusion models. We then introduce the problem definition.

3.1 Sensor Measurement and Network Model

We assume that sensors perform detection by measuring the energy of signals emitted by the target[3]. The energy of most physical signals (*e.g.*, acoustic and electromagnetic signals) attenuates with the distance from the signal source. Suppose sensor i is d_i meters away from the target that emits a signal of energy S. The attenuated signal energy s_i at the position of sensor i is given by

$$s_i = S \cdot w(d_i), \tag{1}$$

where $w(\cdot)$ is a decreasing function satisfying $w(0) = 1$, $w(\infty) = 0$, and $w(x) = \Theta(x^{-k})$. The $w(\cdot)$ is referred to as the *signal decay function*. Depending on the environment, *e.g.*, atmosphere conditions, the signal's path loss exponent k typically ranges from 2.0 to 5.0 [15, 20]. We note that the theoretical results derived in this paper do not depend on the closed-form formula of $w(\cdot)$. We adopt the following signal decay function in the simulations conducted in this paper:

$$w(x) = \frac{1}{1 + x^k}. \tag{2}$$

The sensor measurements are contaminated by additive random noises from sensor hardware or environment. Depending on the hypothesis that the target is absent (H_0) or present (H_1), the measurement of sensor i, denoted by y_i, is given by

$$H_0: \quad y_i = n_i, \tag{3}$$

$$H_1: \quad y_i = s_i + n_i, \tag{4}$$

where n_i is the energy of noise experienced by sensor i. We assume that the noise n_i at each sensor i follows the normal distribution, *i.e.*, $n_i \sim \mathcal{N}(\mu, \sigma^2)$, where μ and σ^2 are the mean and variance of n_i, respectively. We assume that the noises, $\{n_i | \forall i\}$, are spatially independent across sensors. Therefore, the noises at sensors are independent and identically distributed (*i.i.d.*) Gaussian noises. In the presence of target, the measurement of sensor i follows the normal

Table 1: Summary of Notation*

Symbol	Definition
S	original signal energy emitted by the target
μ, σ^2	mean and variance of noise energy
δ	peak signal-to-noise ratio (PSNR), $\delta = S/\sigma$
k	path loss exponent
$w(\cdot)$	signal decay function, $w(x) = \Theta(x^{-k})$
d_i	distance from the target
s_i	attenuated signal energy, $s_i = S \cdot w(d_i)$
n_i	noise energy, $n_i \sim \mathcal{N}(\mu, \sigma^2)$
y_i	signal energy measurement, $y_i = s_i + n_i$
P_F / P_D	false alarm rate / detection probability
α / β	upper / lower bound of P_F / P_D
H_0 / H_1	hypothesis that the target is absent / present
ρ	network density
$\mathbf{F}(p)$	the set of sensors within fusion range of point p
$N(p)$	the number of sensors in $\mathbf{F}(p)$
ϵ	upper bound of target localization error

* The symbols with subscript i refer to the notation of sensor i.

[3]Several types of sensors (*e.g.*, acoustic sensor) only sample *signal intensity* at a given sampling rate. The *signal energy* can be obtained by preprocessing the time series of a given interval, which has been commonly adopted to avoid the transmission of raw data [8, 10, 11, 20, 34].

distribution, *i.e.*, $y_i|H_1 \sim \mathcal{N}(s_i + \mu, \sigma^2)$. Due to the independence of noises, the sensors' measurements, $\{y_i|\forall i, H_1\}$, are spatially independent but *not* identically distributed as sensors receive different signal energies from the target. We define the peak signal-to-noise ratio (PSNR) as $\delta = S/\sigma$ which quantifies the noise level. Table 1 summarizes the notation used in this paper.

The above signal decay and additive *i.i.d.* Gaussian noise models have been widely adopted in the literature of multi-sensor signal detection [2, 5, 8, 20, 24, 27, 29, 34, 37, 40] and also have been empirically verified [15, 20]. In practice, the parameters of these models (*i.e.*, S, $w(\cdot)$, μ, and σ^2) can be estimated using training data. The normal distribution might be an approximation to the real noise distribution in practice. As discussed in Section 5.1, the assumption of *i.i.d.* Gaussian noises can be relaxed to any *i.i.d.* noises.

We consider a network deployed in a vast two-dimensional geographical region. The positions of sensors are uniformly and independently distributed in the region. Such a deployment scenario can be modeled as a stationary two-dimensional Poisson point process. Let ρ denote the density of the underlying Poisson point process. The number of sensors located in a region A, $N(A)$, follows the Poisson distribution with mean of $\rho||A||$, *i.e.*, $N(A) \sim \text{Poi}(\rho||A||)$, where $||A||$ represents the area of the region A. We note that the uniform sensor distribution has been widely adopted in the performance analysis of large-scale WSNs [4, 19, 24, 33, 38]. Therefore, this assumption allows us to compare our results with previous analytical results.

3.2 Data Fusion Model

Data fusion can improve the performance of detection systems by jointly considering the noisy measurements of multiple sensors. There exist two basic data fusion schemes, namely, *decision fusion* and *value fusion*. In decision fusion, each sensor makes a *local* decision based on its measurements and sends its decision to the cluster head, which makes a *system* decision according to the local decisions. The optimal decision fusion rule has been obtained in [5]. In value fusion, each sensor sends its measurements to the cluster head, which makes the detection decision based on the received measurements. In this paper, we focus on value fusion, as it usually has better detection performance than decision fusion [37]. Under the assumptions made in Section 3.1, the optimal value fusion rule is to compare the following weighted sum of sensors' measurements to a threshold (the derivation can be found in Appendix A):

$$Y_{\text{opt}} = \sum_i \frac{s_i}{\sigma} \cdot y_i.$$

However, as sensor measurements contain both noise and signal energy (see (4)), the weight $\frac{s_i}{\sigma}$, *i.e.*, the SNR received by sensor i, is unknown. A practical solution is to adopt equal constant weights for all sensors' measurements [8, 29, 40]. Since the measurements from different sensors are treated equally, the sensors far away from the target should be excluded from data fusion as their measurements suffer low SNRs. Therefore, we adopt a fusion scheme as follows.

For any physical point p, the sensors within a distance of R meters from p form a cluster and fuse their measurements to detect whether a target is present at p. R is referred to as the *fusion range* and $\mathbf{F}(p)$ denotes the set of sensors within the fusion range of p. The number of sensors in $\mathbf{F}(p)$ is represented by $N(p)$. A cluster head is elected to make the detection decision by comparing the sum of measurements reported by member sensors in $\mathbf{F}(p)$ against a detection threshold T. Let Y denote the *fusion statistics*, *i.e.*, $Y = \sum_{i \in \mathbf{F}(p)} y_i$. If $Y \geq T$, the cluster head decides H_1; otherwise, it decides H_0.

We assume that the cluster head makes a detection based on snapshot measurements from member sensors without using temporal samples to refine the detection decision. Note that such a snapshot scheme is widely adopted in previous works on target surveillance [8, 20, 29, 34, 40]. Fusion range R is an important design parameter of our data fusion model. As SNR received by sensor decays with distance from the target, fusion range lower-bounds the quality of information that is fused at the cluster head. In Section 5.2, we will discuss how to choose the optimal fusion range. The above data fusion model is consistent with the fusion schemes adopted in [8, 29, 40]. If more efficient fusion models are employed, the scaling laws proved in this paper still hold as discussed in Section 6.5.

We assume that the target keeps stationary after appearance and the position of a possible target can be obtained through a localization algorithm. For instance, the target position can be estimated as the geometric center of a number of sensors with the largest measurements. Such a simple localization algorithm is employed in the simulations conducted in this paper. The localized position may not be the exact target position and the distance between them is referred to as *localization error*. We assume that the localization error is upper-bounded by a constant ϵ. The localization error is accounted for in the following analyses. However, we show that it has no impact on the asymptotic results derived in this paper.

The above data fusion model can be used for target detection as follows. The detection can be executed periodically or triggered by user queries. In a detection process, each sensor makes a snapshot measurement and a cluster is formed by the sensors within the fusion range from the possible target to make a detection decision. The cluster formation may be initiated by the sensor that has the largest measurement. Such a scheme can be implemented by several dynamic clustering algorithms [6]. The fusion range R can be used as an input parameter of the clustering algorithm. The communication topology of the cluster can be a multi-hop tree rooted at the cluster head. As the fusion statistics Y is an aggregation of sensors' measurements, it can be computed efficiently along the routing path to the cluster head. In this work, we are interested in the fundamental performance limits of coverage under the fusion model and the design of clustering and data aggregation algorithms is beyond the scope of this paper.

3.3 Problem Definition

The detection of a target is inherently stochastic due to the noise in sensor measurements. The detection performance is usually characterized by two metrics, namely, the false alarm rate (denoted by P_F) and detection probability (denoted by P_D). P_F is the probability of making a positive decision when *no* target is present, and P_D is the probability that a present target is correctly detected. In stochastic detection, positive detection decisions may be false alarms caused by the noise in sensor measurements. In particular,

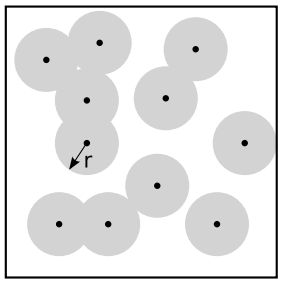

Figure 3: Coverage under the disc model. Sensing range $r = 17\,\mathrm{m}$, which is computed by (7).

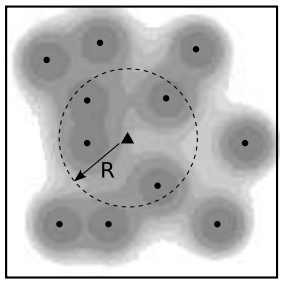

Figure 4: Coverage under the fusion model. Grayscale represents the value of P_D.

although the detection probability can be improved by setting lower detection thresholds, the fidelity of detection results may be unacceptable because of high false alarm rates. Therefore, P_F together with P_D characterize the sensing quality provided by the network. For a physical point p, we denote the probability of successfully detecting a target located at p as $P_D(p)$. Note that P_F is the probability of making positive decision when *no* target is present, and hence is location independent.

Our focus is to study the coverage of large-scale WSNs. We introduce a concept called (α, β)-*coverage* that quantifies the fraction of the surveillance region where P_F and P_D are bounded by α and β, respectively.

DEFINITION 1 ((α, β)-COVERAGE). *Given two constants $\alpha \in (0, 0.5)$ and $\beta \in (0.5, 1)$, a physical point p is* (α, β)-covered *if the false alarm rate P_F and detection probability $P_D(p)$ satisfy*

$$P_F \leq \alpha, \quad P_D(p) \geq \beta.$$

The (α, β)-coverage of a region is defined as the fraction of points in the region that are (α, β)-covered.

The *full coverage* of a region refers to the case where the (α, β)-coverage of the region approaches one, *i.e.*, the false alarm rate is below α and the probability of detecting a target present at *any* location is above β. In practice, mission-critical surveillance applications [11–13, 16] require a low false alarm rate ($\alpha < 5\%$) and a high detection probability ($\beta \gg 50\%$).

We now illustrate the (α, β)-coverage by an example, where $\delta = 1000$ (*i.e.*, $30\,\mathrm{dB}$), $\alpha = 5\%$, $\beta = 95\%$, and $R = 50\,\mathrm{m}$. Fig. 3 and 4 illustrate the coverage under the disc and fusion models, respectively. In Fig. 4, when a target (represented by the triangle) is present, the sensors within the fusion range from it fuse their measurements to make a detection. The gray area is (α, β)-covered, where grayscale represents the value of P_D at each point. As shown in Fig. 3, the covered region under the disc model is simply the union of all sensing discs. As a result, when a high level of coverage is required, a large number of extra sensors must be deployed to eliminate small uncovered areas surrounded by sensing discs. In contrast, data fusion can effectively expand the covered region by exploiting the collaboration among neighboring sensors.

In the rest of this paper, we consider the following problems:

1. Although a number of analytical results on coverage [4, 19, 24, 33, 38, 41–43] have been obtained under the classical disc model, are they still applicable under the definition of (α, β)-coverage which explicitly captures the stochastic nature of sensing? To answer this question, we propose a probabilistic disc model such that the existing results can be naturally extended to the context of stochastic detection (Section 4).

2. How to quantify the (α, β)-coverage when sensors can collaborate through data fusion? Answering this question enables us to evaluate the coverage performance of a network and to deploy the fewest sensors for achieving a given level of coverage (Section 5).

3. What are the scaling laws between coverage, network density, and signal-to-noise ratio (SNR) under both the disc and fusion models? The results will provide important insights into understanding the limitation of analytical results based on the disc model and the impact of data fusion on the coverage of large-scale WSNs (Section 6).

4. COVERAGE UNDER PROBABILISTIC DISC MODEL

As the classical disc model deterministically treats the detection performance of sensors, existing results based on this model [4, 19, 24, 33, 38, 41–43] cannot be readily applied to analyze the performance or guide the design of real-world WSNs. In this section, we extend the classical disc model based on the stochastic detection theory [37] to capture several realistic sensing characteristics and study the (α, β)-coverage under the extended model.

In the *probabilistic disc model*, we choose the sensing range r such that 1) the probability of detecting any target within the sensing range is no lower than β, and 2) the false alarm rate is no greater than α. As we ignore the detection probability outside the sensing range of a sensor, the detection capability of sensor under this model is lower than in reality. However, this model preserves the *boundary* of sensing region defined in the classical disc model. Hence, the existing results based on the classical disc model [4,19,24,33,38,41–43] can be naturally extended to the context of stochastic detection.

We now discuss how to choose the sensing range r under the probabilistic disc model. The optimal Bayesian detection rule for a single sensor i is to compare its measurement y_i to a detection threshold t [37]. If y_i exceeds t, sensor i decides H_1; otherwise, it decides H_0. Therefore, the P_F and P_D of sensor i are given by

$$P_F = \mathbb{P}(y_i \geq t | H_0) = Q\left(\frac{t-\mu}{\sigma}\right), \tag{5}$$

$$P_D = \mathbb{P}(y_i \geq t | H_1) = Q\left(\frac{t-\mu-s_i}{\sigma}\right), \tag{6}$$

where $\mathbb{P}(\cdot)$ is the probability notation and $Q(\cdot)$ is the complementary cumulative distribution function (CDF) of the standard normal distribution, *i.e.*, $Q(x) = \frac{1}{\sqrt{2\pi}} \int_x^\infty \mathrm{e}^{-t^2/2} \mathrm{d}\, t$. As P_D is non-decreasing function of P_F [37], it is maximized when P_F is set to be the upper bound α. Hence the optimal detection threshold can be solved from (5) as $t_{\mathrm{opt}} = \mu + \sigma Q^{-1}(\alpha)$, where $Q^{-1}(\cdot)$ is the inverse function of

$Q(\cdot)$. By replacing $t = t_{\text{opt}}$ and $s_i = S \cdot w(r)$ in (6), we have

$$r = w^{-1}\left(\frac{Q^{-1}(\alpha) - Q^{-1}(\beta)}{\delta}\right), \tag{7}$$

where $w^{-1}(\cdot)$ is the inverse function of $w(\cdot)$. If the target is more than r meters from the sensor, the detection performance requirements, *i.e.*, α and β, cannot be satisfied by setting any detection threshold. Note that a similar definition of sensing range is proposed in [40] for stochastic detection. From (7), the sensing range of a sensor varies with the user requirements (*i.e.*, α and β) and PSNR δ. For instance, the sensing range r is 3.8 m if $\alpha = 5\%$, $\beta = 95\%$, $\delta = 50$ (*i.e.*, 17 dB)[4] and $w(\cdot)$ is given by (2) with $k = 2$. As $w(\cdot)$ is a decreasing function, $w^{-1}(\cdot)$ is also a decreasing function. Therefore, r increases with the PSNR δ according to (7). This conforms to the intuition that a sensor can detect a farther target if the noise level is lower (*i.e.*, a greater δ).

We now extend the coverage of random networks [4, 24] derived under the classical disc model to (α, β)-coverage. Under both the classical and probabilistic disc models, a location is regarded as being covered if it is within at least one sensor's sensing range. Accordingly, the area of the union of all sensors' sensing ranges is regarded as being covered by the network. The coverage of random networks under the classical disc model has been extensively studied based on the stochastic geometry theory [4, 24]. Specifically, the coverage of a network deployed according to a Poisson point process of density ρ is given by

$$c = 1 - \mathrm{e}^{-\rho\pi r^2}. \tag{8}$$

If the sensing range r is chosen by (7), Eq. (8) computes the (α, β)-coverage of a random network under the probabilistic disc model. This result will be used as the basis for studying the impact of data fusion on network coverage in Section 6.

5. COVERAGE UNDER DATA FUSION MODEL

Although the probabilistic disc model discussed in Section 4 captures the stochastic nature of sensing, it does not exploit the collaboration among sensors. In this section, we first derive the (α, β)-coverage under the fusion model, then illustrate the analytical results using numerical examples.

5.1 Deriving Coverage under Data Fusion Model

We have the following lemma regarding the (α, β)-coverage of random networks.

LEMMA 1. *The (α, β)-coverage of a uniformly deployed network under the data fusion model, denoted by c, is given by*

$$c = \mathbb{P}\left(\frac{\sum_{i\in\mathbf{F}(p)} s_i}{\sqrt{N(p)}} \geq \sigma\left(Q^{-1}(\alpha) - Q^{-1}(\beta)\right)\right), \tag{9}$$

where p is an arbitrary physical point in the network.

[4]The PSNR is set according to the measurements from the vehicle detection experiments based on MICA2 [12] and ExScal [13] motes.

PROOF. We first discuss the necessary and sufficient condition that p is (α, β)-covered. When no target is present, all sensors measure *i.i.d.* noises and hence $Y|H_0 = \sum_{i\in\mathbf{F}(p)} n_i \sim \mathcal{N}(\mu N(p), \sigma^2 N(p))$. Therefore, the false alarm rate is $P_F = \mathbb{P}(Y \geq T|H_0) = Q\left(\frac{T-\mu N(p)}{\sigma\sqrt{N(p)}}\right)$, where T is the detection threshold. As P_D is a non-decreasing function of P_F [37], it is maximized when P_F is set to be the upper bound α. Such a scheme is referred to as the Constant False Alarm Rate detector [37]. Let $P_F = \alpha$, the optimal detection threshold can be derived as $T_{\text{opt}} = \mu N(p) + \sigma Q^{-1}(\alpha)\sqrt{N(p)}$.

When the target is present, $Y|H_1 = \sum_{i\in\mathbf{F}(p)} s_i + n_i \sim \mathcal{N}(\mu N(p) + \sum_{i\in\mathbf{F}(p)} s_i, \sigma^2 N(p))$. Therefore, the detection probability at p is given by

$$P_D(p) = \mathbb{P}(Y \geq T|H_1) = Q\left(\frac{T - \mu N(p) - \sum_{i\in\mathbf{F}(p)} s_i}{\sigma\sqrt{N(p)}}\right)$$

By replacing T with T_{opt} and solving $P_D(p) \geq \beta$, we have the necessary and sufficient condition that p is (α, β)-covered:

$$\frac{\sum_{i\in\mathbf{F}(p)} s_i}{\sqrt{N(p)}} \geq \sigma\left(Q^{-1}(\alpha) - Q^{-1}(\beta)\right). \tag{10}$$

As the random network is stationary, the fraction of covered area equals the probability that an arbitrary point is covered by the network [24]. Therefore, the (α, β)-coverage of the network is given by (9). □

As p is an arbitrary point in the network, $N(p)$ is a Poisson random variable, *i.e.*, $N(p) \sim \text{Poi}(\rho\pi R^2)$. Moreover, $\{s_i | i \in \mathbf{F}(p)\}$ are also random variables. However, we have no closed-form formula for computing (9) due to the difficulty of deriving the CDF of $\frac{\sum_{i\in\mathbf{F}(p)} s_i}{\sqrt{N(p)}}$. We now give an approximation to (9) in the following lemma. The proof is given in Appendix B.

LEMMA 2. *Let μ_s and σ_s^2 denote the mean and variance of $s_i | i \in \mathbf{F}(p)$ for arbitrary point p, respectively. The (α, β)-coverage of a uniformly deployed network under the data fusion model can be approximated by*

$$c \simeq Q\left(\frac{\gamma(R) - \rho\pi R^2}{\sqrt{\rho\pi R^2}}\right), \tag{11}$$

where $\gamma(R) = \left(\frac{Q^{-1}(\alpha)\sigma - Q^{-1}(\beta)\sqrt{\sigma_s^2 + \sigma^2}}{\mu_s}\right)^2$.

We note that the formulas of μ_s and σ_s^2 are given by (17) and (18), respectively. As Central Limit Theorem (CLT) is applied in the derivation of (11), this approximation is accurate when $N(p) \geq 20$ [28]. This condition can be easily met in many applications. For example, it is shown in [12] that the detection probability is only about 40% when four MICA2 motes are deployed in a $10 \times 10\,\text{m}^2$ region. Suppose $R = 20$ m and the network density is the same as in [12], $N(p)$ will be about 50. With the approximate formula, we can evaluate the coverage performance of an existing network or compute the minimum network density to achieve the desired level of coverage under the fusion model. Our simulation results in Section 7 show that (11) can provide accurate prediction of coverage under the fusion model. We note that the localization error has little impact on the accuracy of the approximate formula when $R \gg \epsilon$. Recent sensor

network localization protocols can achieve a precision within 0.5 m in large-scale outdoor deployments [36].

We now derive the lower bound of (α, β)-coverage under the fusion model, which will be used in the derivations of scaling laws in Section 6. We denote $F_{\text{Poi}}(\cdot|\lambda)$ as the CDF of the Poisson distribution $\text{Poi}(\lambda)$, which is formally given by $F_{\text{Poi}}(x|\lambda) = \sum_{k=0}^{\lfloor x \rfloor} \frac{\mathrm{e}^{-\lambda}\lambda^k}{k!}$.

LEMMA 3. *The lower bound of (α, β)-coverage of a uniformly deployed network under the data fusion model, denoted by c_L, is given by*

$$c_L = 1 - F_{\text{Poi}}(\Gamma(R)|\rho\pi R^2), \tag{12}$$

where $\Gamma(R) = \left(\frac{Q^{-1}(\alpha)-Q^{-1}(\beta)}{\delta}\right)^2 \cdot \frac{1}{w^2(R+\epsilon)}$. *When $\rho\pi R^2$ is large enough,*

$$c_L = Q\left(\frac{\Gamma(R) - \rho\pi R^2}{\sqrt{\rho\pi R^2}}\right). \tag{13}$$

PROOF. For any point p, $\sum_{i\in\mathbf{F}(p)} s_i \geq S \cdot w(R+\epsilon) \cdot N(p)$, as $s_i \geq S \cdot w(R+\epsilon)$ for any sensor i in $\mathbf{F}(p)$. If $\frac{S\cdot w(R+\epsilon)\cdot N(p)}{\sqrt{N(p)}} \geq \sigma\left(Q^{-1}(\alpha) - Q^{-1}(\beta)\right)$, Eq. (10) must hold. Therefore, by solving $N(p)$, the sufficient condition that p is (α, β)-covered is $N(p) \geq \Gamma(R)$. Moreover, as $N(p) \sim \text{Poi}(\rho\pi R^2)$, we have

$$\begin{aligned} c &= \mathbb{P}(\text{point } p \text{ is } (\alpha,\beta)\text{-covered}) \\ &\geq \mathbb{P}(N \geq \Gamma(R)) \\ &= 1 - F_{\text{Poi}}(\Gamma(R)|\rho\pi R^2). \end{aligned}$$

Therefore, the lower bound of c is given by (12). When $\rho\pi R^2$ is large enough, the normal distribution $\mathcal{N}(\rho\pi R^2, \rho\pi R^2)$ excellently approximates the Poisson distribution $\text{Poi}(\rho\pi R^2)$. Therefore, Eq. (12) can be approximated by (13). □

In the proofs of above lemmas, the fusion statistics Y has a component $\sum_{i\in\mathbf{F}(p)} n_i$. According to the CLT, this component approximately follows the normal distribution if $\{n_i\}$ are *i.i.d.*. Therefore, the assumption of *i.i.d.* Gaussian noises made in Section 3.1 can be relaxed to *i.i.d.* noises that follow any distribution, when the number of sensors taking part in data fusion is large enough. In practice, the accuracy of this approximation is satisfactory when $N(p) \geq 20$ [28]. In particular, the distribution of noise will not affect the asymptotic scaling laws in Section 6, as $N(p)$ is large in the asymptotic scenarios where $c \to 1$.

5.2 Numerical Examples

In this section, we provide several numerical results to help understand the coverage performance under the data fusion model. We adopt the signal decay function given by (2) with $k = 2$. Fig. 5 plots the approximate coverage computed by (11). We can see from Fig. 5 that the coverage initially increases with fusion range R, but decreases to zero eventually. Intuitively, as the fusion range increases, more sensors contribute to the data fusion resulting in better sensing quality. However, as R becomes very large, the aggregate noise starts to cancel out the benefit because the target signal decreases quickly with the distance from the target. In other words, the measurements of sensors far away from the target contain low quality information and hence fusing them leads to lower detection performance. An important question is thus how to choose the optimal fusion range (denoted by R_{opt}) that maximizes the coverage. First, the R_{opt} can be obtained through numerical experiments. Fig. 6 plots the optimal fusion ranges under different network densities, which are obtained by numerically maximizing the coverage. Second, it is possible to obtain the analytical R_{opt} by solving $\frac{\mathrm{d}c}{\mathrm{d}R} = 0$. For instance, when the signal decay function $w(\cdot)$ is given by (2) with $k = 2$, R_{opt} satisfies $\frac{R_{\text{opt}}}{\ln R_{\text{opt}}} = \Theta(\sqrt{\rho})$ and hence R_{opt} increases with network density ρ.

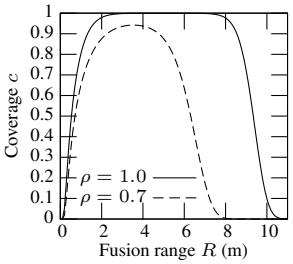

Figure 5: Coverage *vs.* fusion range ($\delta = 4$, $\alpha = 5\%$, $\beta = 95\%$).

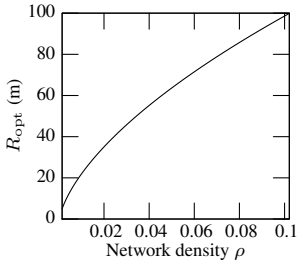

Figure 6: Optimal fusion range *vs.* density($\delta = 100$, $\alpha = 5\%$, $\beta = 95\%$).

6. IMPACT OF DATA FUSION ON COVERAGE

Many mission-critical applications require a high level of coverage over the surveillance region. As an asymptotic case, full coverage is required, *i.e.*, *any* target/event present in the region can be detected with a probability of at least β while the false alarm rate is below α. As a higher level of coverage always requires more sensors, the network density for achieving full coverage is an important cost metric for mission-critical applications.

Under the disc model, the sensing regions of randomly deployed sensors inevitably overlap with each other when a high level coverage is required. According to (8), we have $\mathrm{d}\rho = \frac{1}{\pi r^2} \cdot \frac{1}{1-c} \cdot \mathrm{d}c$. If c is close to 1, a large number of extra sensors (*i.e.*, $\mathrm{d}\rho$) are required to eliminate a small uncovered area (*i.e.*, $\mathrm{d}c$). Moreover, the situation gets worse when c increases. In this section, we are interested in how much network density can be reduced by adopting data fusion. Specifically, we study the asymptotic relationships between the network densities for achieving full coverage under the probabilistic disc and data fusion models. The results provide important insights into understanding the limitation of the disc model and the impact of data fusion on coverage.

6.1 Full Coverage using Fixed Fusion Range

We first study the relationship between the network densities for achieving full coverage under the disc and fusion models when fusion range R is a constant. We have the following theorem.

THEOREM 1. *Let ρ_d and ρ_f denote the minimum network densities required to achieve the (α, β)-coverage of c under the disc and fusion models, respectively. If the fusion range R is fixed, we have*

$$\rho_f = \mathcal{O}\left(\frac{2r^2}{R^2} \cdot \rho_d\right), \quad c \to 1. \tag{14}$$

PROOF. As ρ_f is large to provide a high level of coverage under the fusion model, the lower bound of (α, β)-coverage, c_L, is given by (13) according to Lemma 3. We define $h_1(\rho_f) = \frac{\Gamma(R)}{\sqrt{\pi}R} \cdot \frac{1}{\sqrt{\rho_f}}$, $h_2(\rho_f) = \sqrt{\pi}R \cdot \sqrt{\rho_f}$ and hence $c_L = Q(h_1(\rho_f) - h_2(\rho_f))$. When $\rho_f \to \infty$, $h_2(\rho_f)$ dominates $h_1(\rho_f)$ as $\lim_{\rho_f \to \infty} \frac{h_1(\rho_f)}{h_2(\rho_f)} = 0$. Hence, $c \geq c_L = Q(-h_2(\rho_f)) = Q(-\sqrt{\pi}R \cdot \sqrt{\rho_f})$ when $\rho_f \to \infty$. Define $x = Q^{-1}(c)$. We have $\rho_f \leq \frac{1}{\pi R^2} x^2$ when $c \to 1$.

Under the disc model, by replacing $c = Q(x) = 1 - \Phi(x)$ in (8) and solving ρ_d, we have $\rho_d = -\frac{1}{\pi r^2} \ln \Phi(x)$, where $\Phi(x)$ is the CDF of the standard normal distribution. Hence, we have

$$\lim_{c \to 1} \frac{\rho_f}{\rho_d} \leq \lim_{x \to -\infty} \frac{\frac{1}{\pi R^2} x^2}{-\frac{1}{\pi r^2} \ln \Phi(x)} = -\frac{r^2}{R^2} \lim_{x \to -\infty} \frac{x^2}{\ln \Phi(x)}.$$

As $\lim_{x \to -\infty} \frac{x^2}{\ln \Phi(x)} = -2$ (derived in Appendix C), we have $\lim_{c \to 1} \frac{\rho_f}{\rho_d} \leq \frac{2r^2}{R^2}$. Therefore, the asymptotic upper bound of ρ_f is given by (14). □

Theorem 1 shows that in order to achieve full coverage, ρ_f is smaller than ρ_d if $R > \sqrt{2}r$. According to (7), sensing range r is a constant independent of network density. On the other hand, fusion range R is a design parameter of the fusion model, which is mainly constrained by the communication overhead. In practice, the condition $R > \sqrt{2}r$ can be easily satisfied. For instance, the acoustic sensor on MICA2 motes has a sensing range of 3 m to 5 m if a high performance (*e.g.*, $\alpha = 5\%$ and $\beta = 95\%$) is required [12]. On the other hand, the fusion range can be set to be much larger. For example, Fig. 6 shows that R_{opt} ranges from 5 m to 100 m when network density increases from 1.5×10^{-3} to 0.1. Therefore, according to Theorem 1, the fusion model with the optimal fusion range can significantly reduce network density for achieving a high level of coverage.

6.2 Full Coverage using Optimal Fusion Range

As discussed in Section 5.2, we can obtain the optimal fusion range via numerical experiment or analysis. Data fusion with the optimal fusion range allows the maximum number of informative sensors to contribute to the detection. The scaling law obtained with optimal fusion range will help us understand the maximum performance gain by adopting the data fusion model. The following theorem shows that ρ_f further reduces to $\mathcal{O}(\rho_d^{1-1/k})$ as long as the fusion range is optimal. The proof is given in Appendix D.

THEOREM 2. *Let ρ_d and ρ_f denote the minimum network densities required to achieve the (α, β)-coverage of c under the disc and fusion models, respectively. If the optimal fusion range R_{opt} is adopted, we have*

$$\rho_f = \mathcal{O}\left(\rho_d^{1-1/k}\right), \quad c \to 1. \tag{15}$$

Theorem 2 shows that if the optimal fusion range is adopted, the fusion model can significantly reduce the network density for achieving high coverage. In particular, from Theorem 2, the density ratio $\frac{\rho_f}{\rho_d} = \mathcal{O}(\rho_d^{-1/k}) = 0$ when $c \to 1$, which means ρ_f is insignificant compared with ρ_d for achieving high coverage. Theorem 2 is applicable to the scenarios where the physical signal follows the power law decay with path loss exponent k, which are widely assumed and verified in practice. We note that the path loss exponent k typically ranges from 2.0 to 5.0 [15,20]. In particular, the propagation of acoustic signals in free space follows the inverse-square law, *i.e.*, $k = 2$, and therefore $\rho_f = \mathcal{O}(\sqrt{\rho_d})$.

6.3 Impact of Signal-to-Noise Ratio

In this section, we study the impact of PSNR on the results derived in the previous sections. PSNR is an important system parameter which is determined by the property of target, noise level, and sensitivity of sensors. We have the following corollary.

COROLLARY 1. *For fixed fusion range R, we have*

$$\frac{\rho_f}{\rho_d} = \mathcal{O}(\delta^{2/k}), \quad c \to 1. \tag{16}$$

PROOF. As $w(x) = \Theta(x^{-k})$, $w^{-1}(x) = \Theta(x^{-1/k})$. According to (7), the sensing range $r = \Theta(\delta^{1/k})$. As $\lim_{c \to 1} \frac{\rho_f}{\rho_d} \leq \frac{2r^2}{R^2} = \Theta(\delta^{2/k})$, we have (16). □

Corollary 1 suggests that for a fixed R, the relative cost between the fusion and disc models is affected by the PSNR δ. Specifically, the fusion model requires fewer sensors to achieve full coverage than the disc model if the PSNR is low. On the other hand, the disc model suffices only if the PSNR is *sufficiently* high. Intuitively, sensor collaboration is more advantageous when the PSNR is low to moderate. However, when the PSNR is *sufficiently* high, the detection performance of a single sensor is satisfactory and the collaboration among multiple sensors may be unnecessary.

6.4 Implications of Results

We now summarize the implications of theoretical results derived in this section.

6.4.1 The limitations of disc model

According to Theorem 2, when the required coverage approaches one, ρ_d increases significantly faster than ρ_f, especially for a small decay exponent. For instance, when $k = 2$ (which typically holds for acoustic signals), $\rho_f = \mathcal{O}(\sqrt{\rho_d})$. This result implies that the existing analytical results based on the disc model (*e.g.*, [4, 19, 24, 33, 38, 43]) significantly overestimate the network density required for achieving full coverage. On the other hand, Corollary 1 shows that the disc model may lead to similar or even lower network density than the fusion model if PSNR is sufficiently high. The noise experienced by a sensor in real systems comes from various sources, *e.g.*, the random disturbances in the environment and the electronic noise in sensor circuit. In practice, the PSNRs in the applications based on low-cost sensors are usually low. For instance, the PSNRs in the vehicle detection experiments based on MICA2 [12] and ExScal [13] motes are about 50 (*i.e.*, 17 dB). In such a case, $\rho_d \geq 2\rho_f$ for achieving a high level of coverage if R is set to be greater than 8 m.

6.4.2 Design of data fusion algorithms

Our results provide several important guidelines on the design of data fusion algorithms for large-scale WSNs. First, data fusion is very effective in improving sensing coverage and reducing network density. In particular, Theorem 2 suggests that the performance gain of data fusion increases when the PSNR is lower. Therefore, data fusion should be

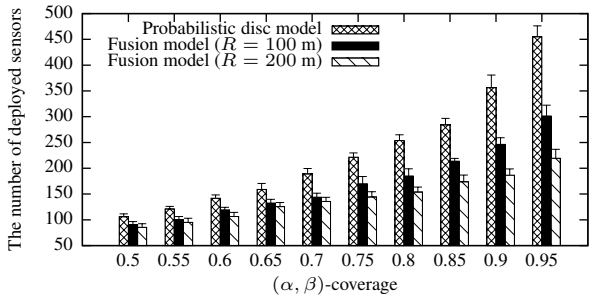

Figure 7: The number of deployed sensors *vs.* achieved (α, β)-coverage.

employed for low-SNR deployments when a high level of coverage is required. Second, Theorems 1 and 2 suggest that fusion range plays an important role in the achievable performance of data fusion. As discussed in Section 5.2, the optimal fusion range that maximizes coverage increases with network density and can be numerically computed. However, a larger fusion range requires more sensors to fuse their measurements resulting in higher communication overhead. Investigating the optimal fusion range under both coverage and communication constraints is left for future work.

6.5 Discussion

We now discuss several issues that have not been addressed in this paper.

The main objective of this paper is to explore the fundamental limits of coverage based on data fusion model in target surveillance applications, in which sensors measure the signals emitted by the target. The proofs of Lemma 1-3 and Theorem 1 are not dependent on the form of the signal decay function $w(\cdot)$. Therefore, these results hold under *arbitrary* bounded decreasing function $w(\cdot)$. However, Theorem 2 and Corollary 1 are only applicable for the applications where the target signal follows the power law decay, *i.e.*, $w(x) = \Theta(x^{-k})$. We acknowledge that most mechanical and electromagnetic waves follow the power law decay in propagation. In particular, in open space, inverse-square law (*i.e.*, $k = 2$) [9] applies to various physical signals such as sound, light and radiation. In our future work, we will extend our analyses to address other decay laws such as exponential decay in diffusion processes [35].

Theorem 1-2 and Corollary 1 give the upper bounds of network density under the fusion model presented in Section 3.2. If more efficient fusion models are employed, the coverage performance will be further improved. In other words, more efficient fusion model can reduce the network density for achieving a certain level of coverage. As a result, the upper bounds of network density derived in this paper still hold. Exploring the impact of efficiency of fusion models on network density is left for future work.

7. SIMULATIONS

In this section, we conduct extensive simulations based on real data traces as well as synthetic data to evaluate the coverage performance in non-asymptotic and asymptotic cases, respectively.

7.1 Trace-driven Simulations

We first conduct simulations using the data traces collected in a real vehicle detection experiment [1]. In the experiments, 75 WINS NG 2.0 nodes are deployed to detect military vehicles driving through the surveillance region. We refer to [11] for detailed setup of the experiments. The dataset used in our simulations includes the ground truth data and the acoustic time series recorded by 20 nodes when a vehicle drives through. The ground truth data include the positions of sensors and the trajectory of the vehicle.

Sensors' sensing ranges under the probabilistic disc model are determined individually to meet the detection performance requirements ($\alpha = 5\%$ and $\beta = 95\%$). The resulted sensing ranges are from 22.5 m to 59.2 m with the average of 43.2 m. Such a significant variation is due to several issues including poor calibration and complex terrain. In our simulation, we deploy random networks with size of $1000 \times 1000\,\mathrm{m}^2$. Each sensor in the simulation is associated with a real sensor chosen at random. For each deployment, we evaluate the (α, β)-coverage under both the disc and fusion models. We divide the region into 1000×1000 grids. Under the disc model, the coverage is estimated as the ratio of grid points that are covered by discs. Under the fusion model, the coverage is estimated as the ratio of (α, β)-covered grid points. Specifically, for a target that appears at a grid point, each sensor makes a measurement which is set to be the energy gathered by the associated real sensor at a similar distance to vehicle in the data trace. A cluster is formed around the sensor with the highest reading, which fuses sensor measurements for detection.

Fig. 7 plots the the number of deployed sensors versus the achieved (α, β)-coverage under various settings. We can see that the disc model suffices if a moderate level of coverage is required. However, the fusion model is more effective for achieving high coverage. In particular, the fusion model with a fusion range of 200 m saves more than 50% sensors when the coverage is greater than 0.75. Moreover, the trend of density ratio also follows $\rho_f = \mathcal{O}(\frac{2r^2}{R^2} \cdot \rho_d)$ derived in Section 6.1. We note that the average number of sensors taking part in data fusion is within 30 and hence will not introduce high communication overhead.

7.2 Simulations based on Synthetic Data

7.2.1 Numerical Settings

In addition to trace-driven simulations, we also conduct extensive simulations based on synthetic data. These simulations allow us to evaluate the theoretical results in a wide range of settings. We adopt the signal decay function in (2) with $k = 2$. Both the mean and variance of the Gaussian noise generator, μ and σ^2, are set to be 1. We set the orginal energy of target, S, to be 4, 50, and 5000, so that the SNRs in the simulations are consistent with several real experiments [7, 11–13].

As proved in Lemma 1, it suffices to measure the probability that a point is covered for evaluating the coverage of the whole network. Hence, we let the target appear at a fixed point p and deploy random networks with size of $4R \times 4R$ centered at p. For each deployment, $P_D(p)$ is estimated as the fraction of succesful detections. The (α, β)-coverage is estimated as the fraction of deployments whose $P_D(p)$ is greater than β.

We also evaluate the impact of localization error by integrating a simple localization algorithm. Specifically, for each

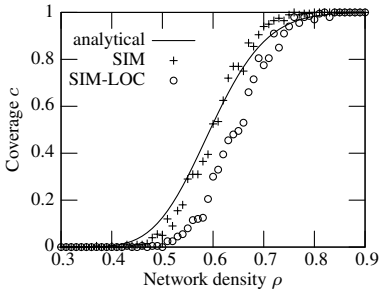

Figure 8: Coverage *vs.* network density ($\delta = 4$, $R = 5\,\mathrm{m}$).

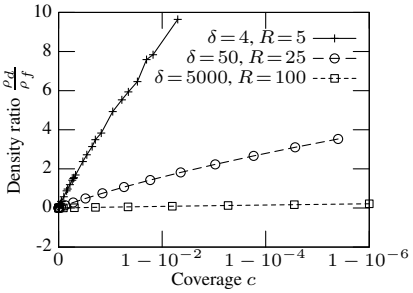

Figure 9: Density ratio $\frac{\rho_d}{\rho_f}$ *vs.* coverage in $\log_{10}$ scale with various PSNRs.

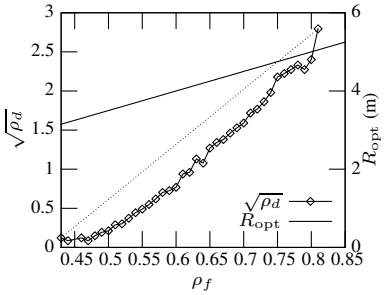

Figure 10: $\sqrt{\rho_d}$ *vs.* ρ_f with optimal fusion range R_{opt} ($\delta = 4$).

detection, if a sensor's reading exceeds $S \cdot w(R) + \mu$, it will take part in the target localization. The target is localized as the geometric center of the sensors participating in the localization.

7.2.2 Simulation Results

We first evaluate the accuracy of the approximate formula given in Lemma 2. Fig. 8 plots the analytical and measured coverage versus network density. The curves labelled with SIM-LOC and SIM represent the measured results with and without accounting for localization error, respectively. We can see that the simulation result matches well the analytical result given by (11). A network density of 0.8 is enough to provide high coverage under the fusion model, where the SNR is very low ($\delta = 4$). When there is localization error, a maximum deviation of about 0.2 from the analytical result can be seen from Fig. 8. The coverage decreases in the presence of localization error as sensors received weaker signals when the target cannot be accurately localized. However, the impact of localization error diminishes when $c \to 1$.

The second set of simulations evaluate the impact of SNR on the asymptotic network densities. Fig. 9 plots the network density ratio $\frac{\rho_d}{\rho_f}$ versus the achieved coverage under various PSNRs, where ρ_d is computed by (8) and ρ_f is obtained in simulations, respectively. The x-axis is plotted in $\log_{10}$ scale. We can see that the density ratio increases with the coverage, *i.e.*, the fusion model becomes more effective for achieving higher coverage. Moreover, the density ratio decreases with the PSNR, which conforms to the result of Corollary 1. For instance, to achieve a high coverage of 0.99, the density ratio $\frac{\rho_d}{\rho_f}$ is about 8 when $\delta = 4$. The density ratio decreases to about 2 when $\delta = 50$. This result shows that data fusion is effective in the scenarios with low SNRs. When $\delta = 5000$, the disc model suffices. These results are consistent with the analysis in Section 6.3.

The third set of simulations evaluate the asymptotic relationship between ρ_d and ρ_f when the fusion range is optimized. In Fig. 10, the X- and Y-axis of each data point represent the required network densities for achieving the same coverage that approaches to one under the disc and fusion models, respectively. Note that the Y-axis is plotted in square root scale. The optimal fusion range R_{opt} plotted in Fig. 10 is computed for each given ρ_f by numerically maximizing (11). We can see from Fig. 10 that the relationship between $\sqrt{\rho_d}$ and ρ_f is convex and therefore conforms to the theoretical result $\rho_f = \mathcal{O}(\sqrt{\rho_d})$ according to Theorem 2. Moreover, R_{opt} increases with ρ_f, which is also consistent with the analysis in Section 5.2.

8. CONCLUSION

Sensing coverage is an important performance requirement of many critical sensor network applications. In this paper, we explore the fundamental limits of coverage based on stochastic data fusion models that jointly process noisy measurements of sensors. The scaling laws between coverage, network density, and signal-to-noise ratio (SNR) are derived. Data fusion is shown to significantly improve sensing coverage by exploiting the collaboration among sensors. Our results help understand the limitations of the existing analytical results based on the disc model and provide key insights into the design and analysis of WSNs that adopt data fusion algorithms. Our analyses are verified through simulations based on both synthetic data sets and data traces collected in a real deployment for vehicle detection.

9. REFERENCES

[1] DARPA SensIT project. `http://www.ece.wisc.edu/~sensit/`.

[2] N. Ahmed, S. S. Kanhere, and S. Jha. Probabilistic coverage in wireless sensor networks. In *LCN*, 2005.

[3] N. Bisnik, A. Abouzeid, and V. Isler. Stochastic event capture using mobile sensors subject to a quality metric. In *MobiCom*, 2006.

[4] P. Brass. Bounds on coverage and target detection capabilities for models of networks of mobile sensors. *ACM Trans. Sen. Netw.*, 3(2), 2007.

[5] Z. Chair and P. Varshney. Optimal data fusion in multiple sensor detection systems. *IEEE Trans. Aerosp. Electron. Syst.*, 22(1), 1990.

[6] W.-P. Chen, J. C. Hou, and L. Sha. Dynamic clustering for acoustic target tracking in wireless sensor networks. *IEEE Trans. Mobile Comput.*, 3(3), 2004.

[7] S. Y. Cheung, S. Coleri, B. Dundar, S. Ganesh, C. W. Tan, and P. Varaiya. A sensor network for traffic monitoring (plenary talk). In *IPSN*, 2004.

[8] T. Clouqueur, K. K. Saluja, and P. Ramanathan. Fault tolerance in collaborative sensor networks for target detection. *IEEE Trans. Comput.*, 53(3), 2004.

[9] D. Davis and C. Davis. *Sound System Engineering.* Focal Press, 1997.

[10] M. Duarte and Y. H. Hu. Distance based decision fusion in a distributed wireless sensor network. In *IPSN*, 2003.

[11] M. Duarte and Y. H. Hu. Vehicle classification in distributed sensor networks. *J. Parallel and Distributed Computing*, 64(7), 2004.

[12] B. P. Flanagan and K. W. Parker. Robust distributed detection using low power acoustic sensors. Technical report, The MITRE Corporation, 2005.

[13] L. Gu, D. Jia, P. Vicaire, T. Yan, L. Luo, A. Tirumala, Q. Cao, T. He, J. Stankovic, T. Abdelzaher, and H. Bruce. Lightweight detection and classification for wireless sensor networks in realistic environments. In *SenSys*, 2005.

[14] C. Gui and P. Mohapatra. Power conservation and quality of surveillance in target tracking sensor networks. In *MobiCom*, 2004.

[15] M. Hata. Empirical formula for propagation loss in land mobile radio services. *IEEE Trans. Veh. Technol.*, 29, 1980.

[16] T. He, S. Krishnamurthy, J. A. Stankovic, T. Abdelzaher, L. Luo, R. Stoleru, T. Yan, L. Gu, J. Hui, and B. Krogh. Energy-efficient surveillance system using wireless sensor networks. In *MobiSys*, 2004.

[17] M. Hefeeda and H. Ahmadi. A probabilistic coverage protocol for wireless sensor networks. In *ICNP*, 2007.

[18] S. Kumar, T. H. Lai, and A. Arora. Barrier coverage with wireless sensors. In *MobiCom*, 2005.

[19] S. Kumar, T. H. Lai, and J. Balogh. On k-coverage in a mostly sleeping sensor network. In *MobiCom*, 2004.

[20] D. Li and Y. H. Hu. Energy based collaborative source localization using acoustic micro-sensor array. *EUROSIP J. Applied Signal Processing*, (4), 2003.

[21] D. Li, K. Wong, Y. H. Hu, and A. Sayeed. Detection, classification and tracking of targets in distributed sensor networks. *IEEE Signal Process. Mag.*, 19(2), 2002.

[22] X. Li, P. Wan, and O. Frieder. Coverage in Wireless Ad Hoc Sensor Networks. *IEEE Trans. Comput.*, 52(6), 2003.

[23] B. Liu, O. Dousse, J. Wang, and A. Saipulla. Strong barrier coverage of wireless sensor networks. In *MobiHoc*, 2008.

[24] B. Liu and D. Towsley. A study on the coverage of large-scale sensor networks. In *MASS*, 2004.

[25] A. Mainwaring, D. Culler, J. Polastre, R. Szewczyk, and J. Anderson. Wireless sensor networks for habitat monitoring. In *WSNA*, 2002.

[26] S. Meguerdichian, F. Koushanfar, M. Potkonjak, and M. B. Srivastava. Coverage problems in wireless ad-hoc sensor networks. In *INFOCOM*, 2001.

[27] S. Meguerdichian, F. Koushanfar, G. Qu, and M. Potkonjak. Exposure in wireless ad-hoc sensor networks. In *MobiCom*, 2001.

[28] NIST/SEMATECH. *e-Handbook of Statistical Methods*.

[29] R. Niu and P. K. Varshney. Distributed detection and fusion in a large wireless sensor network of random size. *EURASIP J. Wireless Communications and Networking*, (4), 2005.

[30] A. Nordio, C. Chiasserini, and E. Viterbo. Quality of field reconstruction in sensor networks. In *INFOCOM*, 2007.

[31] A. Nordio, C. Chiasserini, and E. Viterbo. The impact of quasi-equally spaced sensor layouts on field reconstruction. In *IPSN*, 2007.

[32] S. Ren, Q. Li, H. Wang, X. Chen, and X. Zhang. Design and analysis of sensing scheduling algorithms under partial coverage for object detection in sensor networks. *IEEE Trans. Parallel Distrib. Syst.*, 18(3), 2007.

[33] S. Shakkottai, R. Srikant, and N. Shroff. Unreliable sensor grids: coverage, connectivity and diameter. In *INFOCOM*, 2003.

[34] X. Sheng and Y. H. Hu. Energy based acoustic source localization. In *IPSN*, 2003.

[35] D. Stroock and S. Varadhan. *Multidimensional Diffusion Processes*. Springer, 1979.

[36] C. Taylor, A. Rahimi, J. Bachrach, H. Shrobe, and A. Grue. Simultaneous localization, calibration, and tracking in an ad hoc sensor network. In *IPSN*, 2006.

[37] P. Varshney. *Distributed Detection and Data Fusion*. Springer, 1996.

[38] P.-J. Wan and C.-W. Yi. Coverage by randomly deployed wireless sensor networks. *IEEE/ACM Trans. Netw.*, 14, 2006.

[39] W. Wang, V. Srinivasan, and K. C. Chua. Trade-offs between mobility and density for coverage in wireless sensor networks. In *MobiCom*, 2007.

[40] W. Wang, V. Srinivasan, K.-C. Chua, and B. Wang. Energy-efficient coverage for target detection in wireless sensor networks. In *IPSN*, 2007.

[41] G. Xing, X. Wang, Y. Zhang, C. Lu, R. Pless, and C. Gill. Integrated coverage and connectivity configuration for energy conservation in sensor networks. *ACM Trans. Sen. Netw.*, 1(1), 2005.

[42] T. Yan, T. He, and J. A. Stankovic. Differentiated surveillance for sensor networks. In *SenSys*, 2003.

[43] H. Zhang and J. Hou. On deriving the upper bound of α-lifetime for large sensor networks. In *MobiHoc*, 2004.

APPENDIX

A. OPTIMAL VALUE FUSION RULE

Suppose there are N sensors taking part in the data fusion. The optimal decision rule that minimizes the average cost (*i.e.*, Bayesian decision) is given by the likelihood ratio test:

$$\frac{p(y_1,\ldots,y_N|H_1)}{p(y_1,\ldots,y_N|H_0)} \underset{H_0}{\overset{H_1}{\gtrless}} \frac{P_0(C_{10}-C_{00})}{P_1(C_{01}-C_{11})}.$$

where $P_0 = \mathbb{P}(H_0)$, $P_1 = \mathbb{P}(H_1)$, and C_{ij} is the cost that we decide H_i when the ground truth is H_j. The left-hand side is the likelihood ratio and the right-hand side is the optimal Bayes threshold. As the sensors' measurements are independent Gaussians assumed in Section 3.1, we have

$$\frac{p(y_1,\ldots,y_N|H_1)}{p(y_1,\ldots,y_N|H_0)} = \prod_{i=1}^{N} \frac{p(y_i|H_1)}{p(y_i|H_0)} = \mathrm{e}^{\sum_{i=1}^{N} \frac{2s_iy_i - 2\mu s_i - s_i^2}{\sigma^2}}.$$

Accordingly, the likelihood ratio test becomes

$$\sum_{i=1}^{N} \frac{s_i}{\sigma} \cdot y_i \underset{H_0}{\overset{H_1}{\gtrless}} \frac{1}{2} \sum_{i=1}^{N} \frac{2\mu s_i + s_i^2}{\sigma} + \frac{\sigma}{2} \ln \frac{P_0(C_{10} - C_{00})}{P_1(C_{01} - C_{11})}.$$

Therefore, the optimal fusion statistics for Bayesian decision is $\sum_{i=1}^{N} \frac{s_i}{\sigma} \cdot y_i$ where $\frac{s_i}{\sigma}$ is the received SNR of sensor i.

B. PROOF OF LEMMA 2

PROOF. We first prove that the $\{s_i | i \in \mathbf{F}(p)\}$ are *i.i.d.* for given p and derive the formulas for μ_s and σ_s^2. As sensors are deployed uniformly and independently, $\{d_i | i \in \mathbf{F}(p)\}$ are *i.i.d.* for given p, where d_i is the distance between sensor i and point p. To simplify our discussion, we now temporarily assume that there is no localization error, *i.e.*, $\epsilon = 0$. Therefore, $\{s_i | i \in \mathbf{F}(p)\}$ are *i.i.d.* for given p, as s_i is a function of d_i (defined by (1)). Suppose the coordinates of point p and sensor i are (x_p, y_p) and (x_i, y_i), respectively. The posterior probability density function of (x_i, y_i) is $f(x_i, y_i) = \frac{1}{\pi R^2}$ where $(x_i - x_p)^2 + (y_i - y_p)^2 \leq R^2$. Hence, the posterior CDF of d_i is given by $F(d_i) = \int_0^{2\pi} \mathrm{d}\theta \int_0^{d_i} \frac{1}{\pi R^2} \cdot x \mathrm{d}x = \frac{d_i^2}{R^2}$ where $d_i \in [0, R]$. Therefore, we have

$$\mu_s = \int_0^R s_i \mathrm{d}F(d_i) = \frac{2S}{R^2} \cdot \int_0^R x w(x) \mathrm{d}x, \tag{17}$$

$$\sigma_s^2 = \int_0^R s_i^2 \mathrm{d}F(d_i) - \mu_s^2 = \frac{2S^2}{R^2} \int_0^R x w^2(x) \mathrm{d}x - \mu_s^2. \tag{18}$$

A straightforward approximation is to replace $\sum_{i \in \mathbf{F}(p)} s_i$ in (9) with its mean $\mu_s N(p)$. However, doing so ignores the distribution of $\sum_{i \in \mathbf{F}(p)} s_i$. We approximate $\sum_{i \in \mathbf{F}(p)} s_i$ as a Gaussian random variable according to the CLT, *i.e.*, $\sum_{i \in \mathbf{F}(p)} s_i \sim \mathcal{N}(\mu_s N(p), \sigma_s^2 N(p))$. Note that here we treat $N(p)$ as a constant. When the target is present, $Y | H_1 = \sum_{i \in \mathbf{F}(p)} s_i + \sum_{i \in \mathbf{F}(p)} n_i$. As the sum of two independent Gaussians is also Gaussian, $Y | H_1$ follows the normal distribution, *i.e.*, $Y | H_1 \sim \mathcal{N}(\mu_s N(p) + \mu N(p), \sigma_s^2 N(p) + \sigma^2 N(p))$. Therefore, the detection probability at point p is given by

$$P_D(p) = \mathbb{P}(Y \geq T | H_1) \simeq Q\left(\frac{T - \mu_s N(p) - \mu N(p)}{\sqrt{\sigma_s^2 + \sigma^2} \cdot \sqrt{N(p)}} \right).$$

By replacing T with the optimal detection threshold T_{opt} (derived in the proof of Lemma 1) and solving $P_D(p) \geq \beta$, the condition that p is (α, β)-covered is given by $N(p) \geq \gamma(R)$. The approximate formula of (α, β)-coverage is then given by

$$c \simeq \mathbb{P}(N(p) \geq \gamma(R)) = 1 - F_{\text{Poi}}(\gamma(R) | \rho \pi R^2), \tag{19}$$

where $F_{\text{Poi}}(\cdot | \lambda)$ is the CDF of the Poisson distribution $\text{Poi}(\lambda)$. When $\rho \pi R^2$ is large enough, the Poisson distribution $\text{Poi}(\rho \pi R^2)$ can be excellently approximated by the normal distribution $\mathcal{N}(\rho \pi R^2, \rho \pi R^2)$. Therefore, Eq. (19) can be further approximated by (11). □

C. TWO LIMITS USED IN THE PROOFS OF THEOREMS 1 AND 2

Denote $\phi(x)$ as the probability density function of the standard normal distribution, *i.e.*, $\phi(x) = \frac{1}{\sqrt{2\pi}} \mathrm{e}^{-x^2/2}$. Note that $\Phi'(x) = \phi(x)$ and $\phi'(x) = -x\phi(x)$. For constant $\eta < 0$, we have

$$\begin{aligned}
\lim_{z \to \infty} \frac{z^2}{\ln \Phi(\eta z)} &\overset{(*)}{=} \lim_{z \to \infty} \frac{2z}{\frac{1}{\Phi(\eta z)} \phi(\eta z) \eta} = \frac{2}{\eta} \lim_{z \to \infty} \frac{\Phi(\eta z) z}{\phi(\eta z)} \\
&\overset{(*)}{=} \frac{2}{\eta} \lim_{z \to \infty} \frac{\phi(\eta z) \eta z + \Phi(\eta z)}{-\eta^2 z \phi(\eta z)} = -\frac{2}{\eta^3} \left(\eta + \lim_{z \to \infty} \frac{\Phi(\eta z)}{z \phi(\eta z)} \right) \\
&\overset{(*)}{=} -\frac{2}{\eta^3} \left(\eta + \lim_{z \to \infty} \frac{\phi(\eta z) \eta}{\phi(\eta z) - \eta^2 z^2 \phi(\eta z)} \right) \\
&= -\frac{2}{\eta^3} \left(\eta + \lim_{z \to \infty} \frac{\eta}{1 - \eta^2 z^2} \right) = -\frac{2}{\eta^2},
\end{aligned}$$

where the steps marked by (*) follow from the l'Hôpital's rule. Note that for $\eta < 0$, $\lim_{z \to \infty} \Phi(\eta z) z = 0$ and $\lim_{z \to \infty} z \phi(\eta z) = 0$. By replacing $z = -x$ and $\eta = -1$, we have

$$\lim_{x \to -\infty} \frac{x^2}{\ln \Phi(x)} = -2.$$

D. PROOF OF THEOREM 2

PROOF. We choose R by

$$\frac{\xi}{\pi} \cdot \frac{\Gamma(R)}{R^2} = \rho_f, \tag{20}$$

where ξ is a constant and $\xi > 1$. It is easy to verify that the chosen R is order-optimal for the lower bound of coverage (*i.e.*, c_L). Moreover, it is easy to verify that both the chosen R and $\Gamma(R)$ increase with ρ_f. By replacing ρ_f in (13) with (20), c_L is given by

$$c_L = Q\left(\left(\frac{1}{\sqrt{\xi}} - \sqrt{\xi} \right) \cdot \sqrt{\Gamma(R)} \right) = 1 - \Phi(\eta z),$$

where $\eta = \frac{1}{\sqrt{\xi}} - \sqrt{\xi}$ is a constant and $z = \sqrt{\Gamma(R)}$. Hence we have $c \geq c_L = 1 - \Phi(\eta z)$. According to (8), the network density under the disc model satisfies $\rho_d = -\frac{1}{\pi r^2} \ln(1 - c) \geq -\frac{1}{\pi r^2} \ln \Phi(\eta z)$. Hence, the ratio ρ_f^b / ρ_d where b is a positive constant satisfies

$$\begin{aligned}
\lim_{c \to 1} \frac{\rho_f^b}{\rho_d} &\leq \lim_{R \to \infty} \frac{\left(\frac{\xi}{\pi} \right)^b \cdot \frac{\Gamma^b(R)}{R^{2b}}}{-\frac{1}{\pi r^2} \ln \Phi(\eta z)} \\
&= -\frac{\xi^b r^2}{\pi^{b-1}} \cdot \lim_{z \to \infty} \frac{z^2}{\ln \Phi(\eta z)} \cdot \lim_{R \to \infty} \frac{\Gamma^{b-1}(R)}{R^{2b}} \\
&= \frac{2\xi^b r^2}{\pi^{b-1} \eta^2} \cdot \lim_{R \to \infty} \frac{\Gamma^{b-1}(R)}{R^{2b}}.
\end{aligned}$$

Note that $\lim_{z \to \infty} \frac{z^2}{\ln \Phi(\eta z)} = -\frac{2}{\eta^2}$ (derived in Appendix C) in the above derivation. As $w(x) = \Theta(x^{-k})$ and ϵ is constant, $\Gamma(R) = \Theta(1/w^2(R + \epsilon)) = \Theta((R + \epsilon)^{2k}) = \Theta(R^{2k})$ and hence $\Gamma^{b-1}(R) = \Theta(R^{2kb - 2k})$. Therefore, $\lim_{R \to \infty} \frac{\Gamma^{b-1}(R)}{R^{2b}} = \lim_{R \to \infty} R^{2kb - 2k - 2b}$. If $b \leq \frac{k}{k-1}$, $\lim_{R \to \infty} \frac{\Gamma^{b-1}(R)}{R^{2b}}$ is a constant and hence $\lim_{c \to 1} \frac{\rho_f^b}{\rho_d}$ is upper-bounded by a constant. Hence, we have (15). We note that although the chosen R is not optimal for c, the upper bound given by (15) still holds if R is optimal for c. □